INSTITUTE OF PHYSICS PUBLISHING SUPERCONDUCTOR SCIENCE AND TECHNOLOGY

Supercond. Sci. Technol. **19** (2006) 671–678 doi:10.1088/0953-2048/19/6/042

Peak effect in YBCO crystals: statics and dynamics of the vortex lattice

G Pasquini and V Bekeris

Laboratorio de Bajas Temperaturas, Departamento de Física, FCEN, Universidad de Buenos Aires; CONICET, Argentina

E-mail: pasquini@df.uba.ar

Received 5 April 2006
Published 9 May 2006
Online at stacks.iop.org/SUST/19/671

Abstract

The oscillatory dynamics and quasi-static Campbell regime of the vortex lattice (VL) in twinned $YBa_2Cu_3O_7$ single crystals have been explored at low fields near the peak effect (PE) region by linear and non-linear ac susceptibility measurements. We show evidence that the PE is a dynamic anomaly observed in the non-linear response, and is absent in the Labusch constant derived from the linear Campbell regime. Static properties play a major role however, and we identify two $H(T)$ lines defining the onset and the end of the effect. At $H_1(T)$ a sudden increase in the curvature of the pinning potential wells with field coincides with the PE onset. At a higher field, $H_2(T)$, a sudden increase in linear ac losses, where dissipative forces overcome pinning forces, marks the end of the Campbell regime and, simultaneously, the end of the PE anomaly. Vortex dynamics was probed in frequency dependent measurements, and we find that in the PE region, vortex dynamics goes beyond the description of a power law with a finite creep exponent for the constitutive relation.

1. Introduction

The peak effect (PE) in the critical current density (J_c) in both low and high temperature superconductors has been the subject of a large amount of experimental and theoretical work in the last decade. An anomalous increase is observed above an onset field B_{on} or temperature T_{on}, until J_c reaches a maximum at B_p (or T_p) above which a fast decrease in the measured critical current density occurs, just before reaching either the melting or the upper critical field line.

The origin and nature of this phenomenon are still controversial issues. A unified phenomenological picture based on an order–disorder (O–D) transition for the vortex lattice (VL) from a quasi-ordered Bragg glass (BG) to a disordered phase with increasing topological defects, using the Lindemann criterion has been developed [1], and explains a large amount of experimental results. However, the underlying physics and the nature of this transition is still controversial. Since the first description by Larkin and Ovchinnikov [2], several theoretical pictures have been proposed: the crucial role of dislocations and its consequence in VL dynamics in the PE region was highlighted [3–5]. Recently, a scenario where VL shows no order–disorder phase transition but a continuous transformation to an amorphous state has been proposed [6]: in this picture the PE arises from a change in the dynamics (possible jamming) of vortex matter. Other authors [7] claim that a change in the pinning regime is the origin of the PE. A first-order melting transition from a solid to a liquid VL has also been claimed to be the origin of the PE [8–11]. Probably, the large collection of proposed models are a consequence of the different nature of the PE in the various materials, as is becoming clear from the increasing amount of experimental evidence.

In traditional superconductors, neutron diffraction experiments show a clear change in the structure factor of the VL indicating an O–D transition [12]; the thermal hysteresis observed in this transition should indicate a first-order character. In $NbSe_2$, experiments of magnetization assisted by a shaking ac field [8], as well as transport measurements in the Corbino geometry [9], suggest a first-order transition. Surprisingly, experiments of Bitter decoration [13] show that the disordered VL is not an amorphous (or a pinned liquid) state but a polycrystal. Several works indicate a crucial role of the dynamics of the VL in the PE in this material: a change from an elastic to a dislocation mediated plastic regime [14] and a collective to individual pinning transition [15] at the onset of the PE have been proposed.

In high temperature superconductors (HTSs), the results are still more controversial. In BSCCO samples, the existence of a first-order transition at the PE has been established by experiments of differential magneto-optics (MO) [10], and supported by local magnetization measurements [11]. However, the crucial role of dynamics and creep in the PE, evidenced by the time dependent results, has been known for a long time [16]. The dramatic decrease in the measured J_c before the onset of the PE should be mainly due to creep effects, but it seems to be a precursor to a genuine change in the elastic properties of the VL that reduces the vortex correlation length causing the PE [17]. Recently, direct observation by MO imaging of the magnetic induction profile in the vicinity of the PE, shows a larger J_c in the outer region of the samples, that some authors ascribe to a transient metastable disordered vortex phase penetrating through the sample surface [18], and others to a coexistence between two bulk phases in a local first-order transition [19].

In non-layered HTSs, a direct observation of a VL transition from a BG to a short correlated vortex glass phase (VG) at B_{on} has recently been reported in the LSCO system by muon spin resonance [20].

In the case of YBCO crystals, the first observation of the PE was made more than 10 years ago [21]. However, at the present time the role of disorder and twins in the occurrence of the PE is controversial, and not completely understood [22, 23], and fundamental discussions describing a thermodynamic [24] or a dynamic picture are not settled. In ultrapure samples, an unusually giant and abrupt PE in the non-linear ac susceptibility has been reported [25]. The influence of doping in the VL phase diagram in untwinned YBCO crystals seems to be crucial [26]: by very subtly modifying the oxygen content in the samples, the first-order melting transition [27] from a Bragg glass to a liquid disappears and a transition from a vortex glass to a slush (pinned liquid) [28] phase and then to a liquid has been proposed.

Interestingly, VL history effects are concurrently observed in the PE region in a wide range of superconducting materials, and are probably closely related to the same kind of phenomena. In fact, in the vicinity of the PE, both the mobility of the VL and the measured J_c are found to be dependent on the dynamical history of the sample in both low T_c [9, 29] and high T_c [23, 30, 31] materials. In this framework, a great amount of work was devoted to understand if this phenomenology is dominated by surface or bulk pinning properties. In $NbSe_2$ [9] and BSCCO [32, 33] samples, surface and geometrical barriers seem to play a fundamental role. However, in materials with moderate anisotropy and a high density of pinning centres, as is the case of well oxygenated twinned YBCO, transport properties at $H_{dc} \gg H_{c1}$ are generally well described by bulk pinning forces.

In ac susceptibility experiments, the PE is observed as an anomalous increase in shielding capability or a decrease in losses, also usually interpreted as an anomalous decrease in VL mobility. Recent experiments in YBCO crystals, have shown that the mobility of the VL increases after assisting the system with a symmetric ac field (or current) [31] of moderate amplitude [34]. On the other hand, when vortices are assisted by an asymmetric ac field, the VL becomes less mobile [31]. This salient feature indicates that these effects cannot be ascribed to an equilibration process, but have their origin in the oscillatory character of vortex dynamics.

In our recent work, the solid VL was prepared with different dynamic histories and explored in the linear Campbell regime, using a very small ac field. We have shown that the dynamic history not only determines the degree of mobility, but also directly modifies the effective pinning potential wells, leading to different history dependent static VL configurations (VLCs) [35, 36]. However, in samples where the PE is clearly displayed in the non-linear response, the anomaly (understood as the non-monotonous T dependence) is absent in the Campbell regime [23, 36, 37]. We think that this fact is a key point to understand the nature of the PE.

In this paper, we present new results that will throw light onto this controversial subject. We explore the static and dynamic behaviour of the vortex lattice in YBCO crystals with the dc magnetic field tilted out of the twin boundaries. By performing sensitive linear and non-linear ac susceptibility measurements, we compare the behaviour of VL mobility and the effective pinning potential wells in the region of the PE, at low fields and high temperatures. Assisted by large enough ac fields, vortices perform inter-valley motion and the non-linear penetration depth is directly related to the vortex mobility and the measured critical current density, while for the lower amplitudes, intra-valley motion dominates and the shape of the effective pinning potential well is probed. From our present results, the PE in YBCO crystals originates from a drastic change in the dynamics of the VL. This dynamic change is correlated with a genuine modification in the dependence of the Labusch constant with magnetic field, probably due to a continuos increase in the amount of dislocations.

The paper is organized as follows. In section 2 the experimental array and the numerical procedure followed to analyse the Campbell regime are described. Results and discussions are presented in section 3 and conclusions are drawn in section 4.

2. Methodology

2.1. Experimental array

The samples used were $YBa_2Cu_3O_7$ twinned single crystals [38] (typical dimensions 0.6 × 0.6 × 0.02 mm) with $T_c \sim 92$ K at zero dc field and $\Delta T_c \sim 0.3$ K (10%–90% criterion), in accordance with slightly underdoped crystals. The results shown in this work correspond to a roughly quadrangular shaped sample with a critical temperature (defined as the middle point of the linear ac susceptibility transition at 0 dc field) $T_c = 91$ K. Similar studies have been performed in two other samples, and showed a similar phenomenology.

Global ac susceptibility measurements were carried out with the usual mutual inductance technique. The static magnetic field H_{dc} is provided by a magnet that can be rotated relative to the sample, and was oriented out of all the groups of twin planes. The measuring ac field is parallel to the crystal c axis. All the experimental curves of χ'' and χ' at each amplitude and frequency were normalized by the same factor, corresponding to a total step $\Delta\chi' = 1$ between the normal and superconducting response with $H_{dc} = 0$.

2.2. Numerical procedure

The complex *linear* ac susceptibility $\chi = \chi' + i\chi''$ is characterized to be h_a independent. In a general case, the linear ac response is determined by the complex frequency dependent penetration depth $\lambda_{ac}(f) = \lambda_R + i\lambda_I$ [40]. The function $\chi(\lambda_{ac})$ depends on the sample geometry.

In the particular case of the *linear* frequency independent Campbell regime [39], dissipative processes are negligible compared with the pinning forces and therefore the imaginary penetration depth $\lambda_I \ll \lambda_R$. The restoring force per unit length per vortex is $f_p = -\alpha_L u(r)$, where u is the mean displacement of the vortices in the position r, and α_L is the curvature of the pinning potentials or Labusch constant. In this regime, vortices oscillate inside their effective pinning potential wells without modifying the configuration of the system.

To evaluate λ_R and α_L in the Campbell regime, we approximated our experimental geometry by a thin disc of radius R and thickness δ in a transverse ac magnetic field. We used the numerical solution developed by Brandt [41, 42], in which χ is determined by the adimensional parameter λ_{ac}/D, where $D = (\delta R/2)^{1/2}$ is the characteristic length of the sample. In the Campbell regime $\lambda_R = (\lambda_L^2 + \lambda_c^2)^{1/2}$, where λ_L and $\lambda_c = (\phi_0 B/4\pi\alpha_L)^{1/2}$ are the London and Campbell penetration depths respectively and ϕ_0 and B are the flux quantum and the magnetic induction [40]. When the phase $\varepsilon = \lambda_I/\lambda_R \ll 1$, to first-order in ε, we obtain

$$\chi' + i\chi'' = -1 + f(\lambda_R/D) + i\varepsilon g(\lambda_R/D) \qquad (1)$$

where f and g are functions of the adimensional variable λ_R/D [41, 42]. Therefore, in this limit, the inductive component of the ac susceptibility χ' is determined by the experimental geometry and the adimensional parameter λ_R/D, and the results are frequency independent. We can obtain λ_R by inverting the real part of equation (1):

$$\lambda_R/D = f^{-1}(\chi' + 1) \qquad (2)$$

and considering $B \sim H$

$$\alpha_L = \frac{\phi_0 H}{4\pi(\lambda_R^2 - \lambda_L^2)}. \qquad (3)$$

The normalized London penetration depth λ_L/D was estimated by extrapolating to $H = 0$ the $(\lambda_R/D)^2(H)$ curves (for further numerical details, see [42]). Note that the α_L obtained from equation (3) is the pinning potential curvature evaluated per unit length, per vortex.

The phase ε can easily be estimated from equation (1) and the experimental values of χ' and χ'' as

$$\varepsilon = \frac{\chi''}{g(\frac{\lambda_R}{D}(\chi'))}. \qquad (4)$$

3. Results and discussion

The general behaviour of the peak effect varying the applied ac field is depicted in figure 1, where curves of $\chi''(T)$ (figure 1(a)) and $\chi'(T)$ (figure 1(b)) are shown for various h_a. All curves were measured at $f = 30$ kHz in a warming process, from a VLC prepared by cooling the sample in a dc field $H_{dc} =$ 2000 Oe without any applied ac field ($ZF_{ac}CW$). For high amplitudes, a clear PE with a minimum in χ' at the temperature T_p is displayed. Below T_p, for the lower amplitudes, a linear (i.e. h_a independent) response holds with a very small dissipation. As can be observed, no PE is present in this regime.

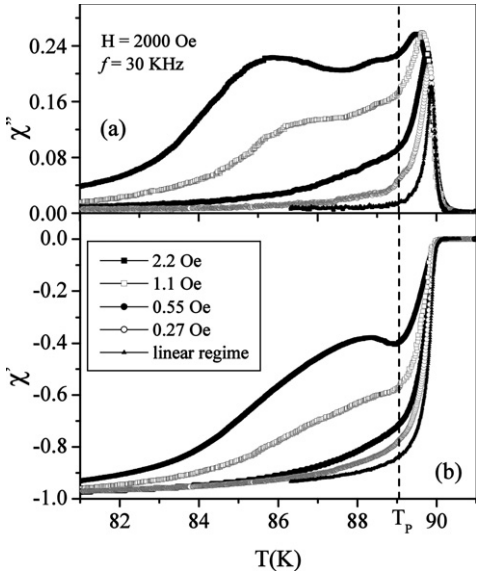

Figure 1. ac susceptibility components $\chi''(T)$ in (a) and $\chi'(T)$ in (b) in a $ZF_{ac}CW$ warming process (see text) for different ac measuring fields at $f = 30$ kHz and $H_{dc} = 2000$ Oe. The PE with a minimum in $\chi'(T)$ at T_p is well established for the non-linear response at high ac measuring field, while it is absent in the linear regime at low ac field.

In the case of flat platelet samples in perpendicular ac fields, we should first elucidate whether geometrical-barrier (GB) dominated VL response [33] or bulk pinning dominated VL response describes our results. In the case of geometrical-barrier (GB) VL response [33], for a given h_a, a maximum in the non-linear χ'' is expected at a dc field $H_0 \sim H_p^2(T)/h_a$, where H_p is the first flux entry penetration magnetic field. At $H_{dc} \ll H_0$, a linear reversible response arising from GBs should hold.

The following arguments discard this option in the present situation. The calculated temperature where $H_0 \sim H_{dc} =$ 2000 Oe for an ac field $h_a = 2.2$ Oe, is $T \sim 26$ K, well below the temperature where the peak in χ'' is observed in figure 1 (curve with black squares). Additionally, the H_{dc} fields where the χ'' peaks are actually observed at different temperatures, are around 100 times higher than the calculated $H_0(T)$. Consistently, in our past work, memory effects in the non-linear ac regime in twinned YBCO crystals have been successfully described within a bulk critical state model [30, 31]. Therefore, we discard GBs as a possible description for the observed non-linear response.

Let us now analyse the linear response. Calculated $H_0(T)$ for the smallest ac field, $h_a = 40$ mOe (linear regime), results to be smaller than the applied field $H_{dc} = 2000$ Oe in the whole temperature range shown in figure 1. The observed linear response therefore holds for $H_{dc} > H_0$, and then cannot be ascribed to GBs. We therefore consistently assume bulk pinning in what follows.

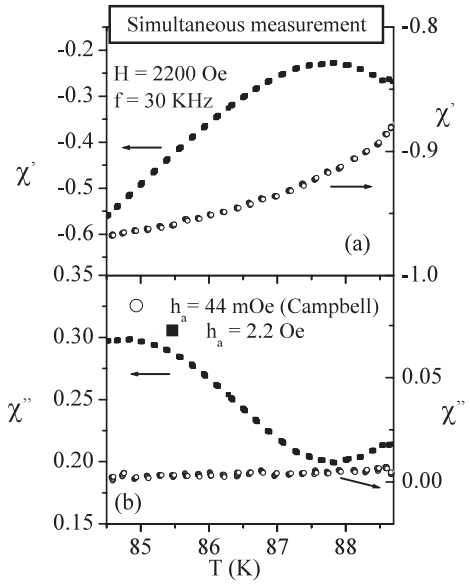

Figure 2. $\chi'(T)$ and $\chi''(T)$ in a unique $ZF_{ac}CW$ warming process for $H_{dc} = 2200$ Oe, switching alternatively from high ($h_a = 1.2$ Oe, full squares, left axis) to low ($h_a = 44$ mOe, open circles, right axis) measuring field amplitudes, at $f = 30$ kHz. Although inter-valley vortex excursions in the non-linear regime (where the PE is observed) allow to explore different VL configurations, the PE is absent in the linear regime.

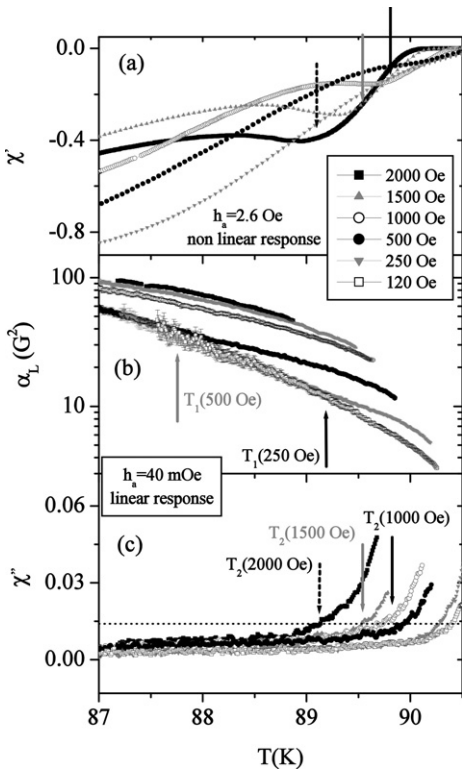

Figure 3. (a) Non-linear $\chi'(T)$, showing the PE for different H_{dc}. (b) $\alpha_L(T)$ in logarithmic scale for different H_{dc}. (c) Linear $\chi''(T)$ indicating the Campbell regime range ($\chi''(T) \sim 0$). Upward arrows in panel (b) indicate $T_1(H_{dc})$ (T_1(500 Oe) grey and T_1(250 Oe) black arrows), where α_L starts to increase with H (see text). Downward arrows in panels (a) and (c) show $T_2(H_{dc})$ (T_2(2000 Oe) dashed arrows, T_2(1500 Oe) full grey arrows and T_2(1000 Oe) full black arrows), where the linear $\chi''(T)$ starts to grow (see text).

The phase $\varepsilon(T)$ has been calculated from the linear curves $\chi'(T)$ and $\chi''(T)$ using equation (4). For the sample shown in figure 1, below T_P, there is a constant phase $\varepsilon \sim 0.07 \pm 0.02$. We also confirmed that below this temperature χ' is frequency independent in the kHz range. These three features: amplitude and frequency independence and very small phase, together with the arguments exposed above against a surface linear response, allow us to state that, below T_P, the Campbell regime holds.

As was pointed out in the introduction, above the onset of the PE a more disordered (and more pinned) VL is expected. Changes in the number and distribution of VL dislocations may affect both static and dynamic properties. However, results from figure 1 indicate that the pinning static properties are not so strongly affected as to produce a PE anomaly, even though the VL mobility is drastically modified.

A first argument for the absence of the PE in the linear response is the fact that changes in the VL topology could be related to very small changes in the Labusch constant, impossible to detect with our experimental technique. We rule out this possibility: in [35] and [36], we have explored the pinning potential corresponding to different VLCs resulting after various protocols or dynamical histories. A clear difference in the penetration depth of the various VLCs has been observed. Therefore, we have shown that we are able to measure changes in λ_R (i.e. in α_L) that can only have their origin in a different VL topology (i.e. a change in the number or distribution of dislocations), and we have the sensitivity to measure that difference.

A possible second explanation for the observed behaviour could be the nature of the Campbell regime. In this regime, vortices remain oscillating around a pinning position, and can only move in a very slow thermal relaxation process [36]. Vortices cannot perform large excursions and therefore most of the VLCs are not accessible. To test this possible scenario, we explored the linear response allowing vortices to alternatively move out of their pinning sites. To achieve this, we performed simultaneous measurements in the linear and non-linear regime alternatively applying high and low measuring ac field amplitudes. With the higher amplitude (non-linear measurement), vortices move and may reorganize in different VLCs. With the small amplitude (linear measurement), the Labush constant corresponding to the attained configuration is measured.

In figure 2, curves for $\chi''(T)$ and $\chi'(T)$ in a unique $ZF_{ac}CW$ warming process at $H_{dc} = 2200$ Oe, switching alternatively from high 1.2 Oe (non-linear) to low 44 mOe (linear) measuring h_a amplitudes at 30 kHz, are shown. Even if vortices move out of their pinning sites (and explore different VLCs) when forced by a larger ac excitation that drives the non-linear response, the temperature dependence of the linear χ' (right axis in the figure) remains monotonous.

Motivated by this striking fact, we have performed an exhaustive comparison of the linear and non-linear behaviour in the PE region. In figure 3, non-linear (top panel) and linear (lower panels) response as a function of temperature at various dc fields are compared. Figure 3(a) shows non-linear $\chi'(T)$

for various $ZF_{ac}CW$ warming processes. In all of the cases, the PE is present. In figure 3(b) the calculated $\alpha_L(T, H_{dc})$ is plotted in logarithmic scale as a function of temperature for the different dc fields. No dramatic changes are observed in the T dependence of the pinning potential curvature, α_L, for any dc field. In figure 3(c) the linear $\chi''(T)$ is displayed. By inspecting the figure however, two characteristic temperatures are observed. At a first temperature we denominate $T_1(H_{dc})$ (see upward arrows in panel (b)) there is a subtle modification in the curvature of $\alpha_L(T)$ at fixed field, that leads to a change in the dependence of $\alpha_L(H)$ at fixed temperature. Below this temperature, α_L seems to become very weakly dependent on magnetic field, in the range $H \leqslant H_{dc}$ within our experimental resolution, whereas above $T_1(H_{dc})$, α_L clearly grows with H for $H \geqslant H_{dc}$. Upward arrows in the figure indicate T_1 for the lower fields: $T_1(500\ \text{Oe}) \sim 87.75$ K (full grey arrow) and $T_1(250\ \text{Oe}) \sim 89.1$ K (full black arrow). At constant H_{dc}, because all the superconducting parameters involved in pinning decrease, the Labusch parameter decreases smoothly and monotonically with temperature in the whole temperature range, but at $T_1(H_{dc})$ the decrease becomes slower, producing a qualitative change in $\alpha_L(H)$ in the PE region. We point out that we are not able to measure $\alpha_L(T)$ at low temperatures and/or lower magnetic fields with our technique, because λ_C becomes too small. Therefore, we are not able to determine the dependence of $\alpha_L(H)$ for $H < H_1$ and the corresponding $T_1(H_{dc})$ for the higher fields lies outside to the left of the measured range.

At a higher temperature $T_2(H_{dc})$, there is a sudden increase in the linear χ'' shown in figure 3(c) (see downward arrows), indicating the end of the Campbell regime and the onset of dissipative mechanisms. We fixed $\chi'' = 0.014$ that corresponds approximately to a phase $\varepsilon \sim 0.07$ as a criterion to define T_2. Downward arrows in figure 3(c) show $T_2(2000\ \text{Oe}) = 89.1$ K (dashed arrows), $T_2(1500\ \text{Oe}) = 89.55$ K (full grey arrows) and $T_2(1000\ \text{Oe}) = 89.8$ K (full black arrows). Note that $T_2(H_{dc})$ is just above the minimum in the non-linear $\chi'(T)$ shown in the top panel, and coincides with the end of the PE.

To better examine the field dependence, data in figure 3 at a few selected temperatures have been plotted in figure 4 as a function of the applied dc magnetic field. The comparison of linear (lower panels) and non-linear response (top panel) is shown. In figure 4(a) the non-linear $\chi'(H)$ with a broad PE in dc field for the highest temperatures is shown. In figure 4(b) values of $\alpha_L(H)$ are shown in logarithmic scale. In figure 4(c) the linear $\chi''(H)$ is displayed. Note that the highest temperatures were selected to match with T_1 or T_2 for some of the measured fields (e.g. 87.75 K $\sim T_1(500\ \text{Oe})$, 89.1 K $\sim T_1(250\ \text{Oe}) = T_2(2000\ \text{Oe})$, 89.55 K $= T_2(1500\ \text{Oe})$, 89.8 K $= T_2(1000\ \text{Oe})$).

The same arrows from figure 3 that indicated $T_1(H_{dc})$ and $T_2(H_{dc})$, are shown in figure 4, now indicating $H_1(T)$ and $H_2(T)$. We identify two characteristic magnetic fields: at a first magnetic field $H_1(T)$ we find a sudden change in the dependence of $\alpha_L(H)$ that increases faster with field above $H_1(T)$, as was anticipated in figure 3(b). Coincidently, the rate of increase of the non-linear $\chi'(H)$ begins to be reduced. The last fact implies a reduction in the rate of increase in the VL mobility and/or a reduction in the rate of decrease

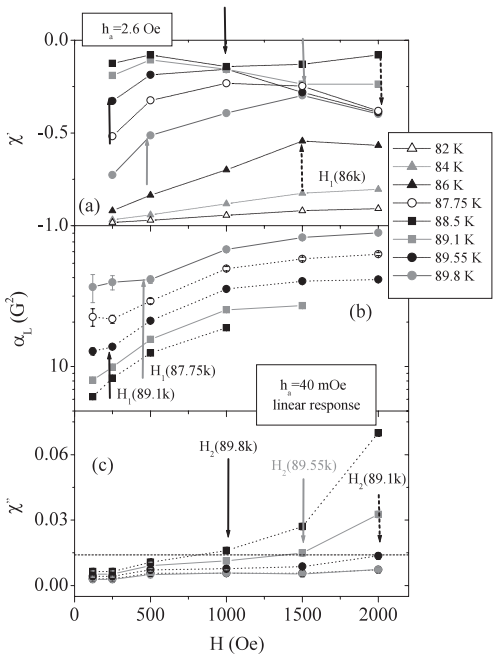

Figure 4. (a) Non-linear $\chi'(H)$ showing a broad PE for different selected temperatures. (b) $\alpha_L(H)$ and error bars (see text) for different T in logarithmic scale. (c) Linear $\chi''(H)$ indicating the Campbell regime range ($\chi''(H) \sim 0$). Upward arrows in panel (b) are the same upward arrows shown earlier in figure 3 indicating $H_1(T)$ ($H_1(89.1\ \text{K}) \sim 250$ Oe, $H_1(87.75\ \text{K}) \sim 500$ Oe full grey and black arrows), where $\alpha_L(H)$ begins to increase strongly with field, setting the onset of the PE in the non-linear $\chi'(H)$. $H_1(86\ \text{K}) \sim 500$ Oe is estimated (see text). Downward arrows in panels (a) and (c) are the same downward arrows of figure 3. They indicate $H_2(T)$ ($H_2(89.8\ \text{K}) \sim 1000$ Oe full black, $H_2(89.55\ \text{K}) \sim 1500$ Oe full grey and $H_2(89.1\ \text{K}) \sim 2000$ Oe dashed arrows), where the Campbell regime is lost and the minimum in the non-linear $\chi'(H)$ occurs. In all cases, the lines are a guide to the eye.

of the measured frequency dependent $J_c(H, T, f)$, producing the onset of the PE. The upward arrows in figure 4 indicate: $H_1(89.1\ \text{K}) \sim 250$ Oe (full black arrows) and $H_1(87.75\ \text{K}) \sim 500$ Oe (full grey arrows). By inspecting figure 4(a), we find an additional $H_1(T)$ in the range of low temperatures, where α_L is not measurable, by approximately identifying the onset of the PE. The dashed grey upward arrow shows $H_1(86\ \text{K}) \sim 1500$ Oe.

To analyse the upper bound of the PE, we refer now to panel (c) in figure 4, where at $H_2(T)$ the linear χ'' grows up to the limit criterion and the Campbell regime is lost. This is an indication that vortices start moving in a highly dissipative regime. Coincidently, the non-linear $\chi'(H)$ in figure 4(a) displays a broad minimum identifying the end of the PE. Downward arrows in the figure show: $H_2(89.8\ \text{K}) \sim 1000$ Oe (full black arrows), $H_2(89.55\ \text{K}) \sim 1500$ Oe (full grey arrows) and $H_2(89.1\ \text{K}) \sim 2000$ Oe (dashed arrows). Therefore, the PE region where the anomaly in the non-linear response develops, occurs between the fields H_1 and H_2.

The growth of α_L with H above H_1 may be related to a reduction of the correlation volume due to the increase of the number of VL defects in the PE region. On the other hand, the collapse of the Campbell regime at H_2, indicates that above

this field, dissipative forces prevail over pinning forces in the linear regime. We interpret this fact as a signature of a phase transition to an unpinned liquid phase.

The proposed picture to explain the above results is the following: at this range of temperature and fields, a bundle regime is expected in the framework of the collective pinning theory. Both J_c and α_L are expected to decrease with an increasing correlation volume V_c. As V_c increases with magnetic field, a decrease in α_L with field is predicted. This is probably what happens below $H_1(T)$, but as was mentioned above, our technique has no sensitivity to measure the field dependence of α_L when λ_C becomes too small. This approach would be valid for a VL free of dislocations, or where the mean distance between dislocations was much larger that the typical correlation distance. We argue that for $H > H_1(T)$ the VL softens and there is a continuous increase in the number of VL defects producing a decrease in the correlation volume and an increase in the Labusch constant with dc field. This mechanism competes with the intrinsic decrease of α_L with temperature, but is not strong enough to overcome it.

Therefore, the anomaly observed in the non-linear penetration depth with temperature, cannot be ascribed only to the softening of the VL, allowing a better accommodation to the pinning centres. The increase in VL defects produces a drastic change in the dynamics and/or creep mechanism, and gives rise to the observed PE anomaly in ac susceptibility in the non-linear response.

As was already pointed out [16, 17], a dynamic origin for the PE should be related to time dependent phenomena. In a continuum description, the dynamics of the VL is directly related with the constitutive relation between the electric field E and the local time dependent current density J. In an ac susceptibility experiment $h_a \ll H$ and $B \sim H$, then the constitutive relation $E(J)$ is expected to depend only on the applied magnetic field and temperature, that together with the sample geometry determines the $\chi''(\chi')$ curves. However, the increasing evidence of history effects in VL dynamics should lead, within this framework, to include history effects in parameters contained in the constitutive relation.

Well known microscopic models for vortex dynamics [7] yield a current density dependent activation energy given by $U(J) = U_0[(J_c/J)^\mu - 1]/\mu$, where $\mu > 0$, $J_c(B, T)$ is the critical current density and $U_0(B, T)$ is the energy scale for the barriers. For thermal creep, $E(J) = E_c \exp(-U(J)/kT)$, where k is the Boltzmann constant. For small values of μ, a suitable approximation for the activation energy is [7] $U(J) \approx U_0 \ln(J_c/J)$, that leads to the well known power law dependence constitutive relation:

$$E(J) = E_c(J/J_c)^n. \tag{5}$$

The exponent $n = U_0/kT$, is field and temperature dependent, and the critical current density J_c is defined with the voltage criterium E_c. Theoretical curves for $\chi''(\chi')$ were calculated in [41] for a type II superconducting thin disc with the power law constitutive relation given above. In this model, $\chi''(\chi')$ is predicted to depend only on the exponent n and the non-linear ac penetration depth. If equation (5) holds, experimental points are expected to lie in a curve that corresponds to a given n. The limit $n = 1$ corresponds to the ohmic flux flow (FF) response, and $n \to \infty$ to an ideal Bean

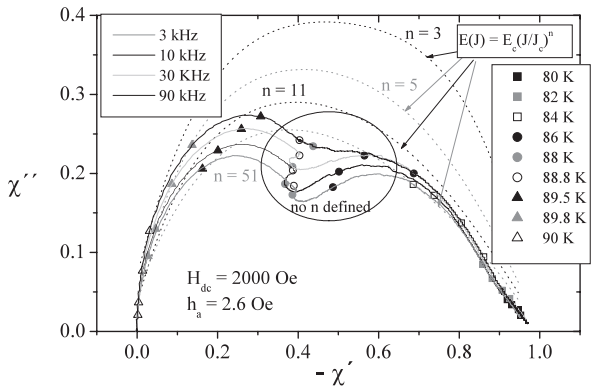

Figure 5. $\chi''(\chi')$ plot. Dotted lines are calculations of ac susceptibility for a disc including creep, for the constitutive relation $E(J) = E_0(J/J_c)^n$ describing logarithmic current dependent creep barriers. The full lines are the curves for different frequencies $f = 3$, 10, 30 and 90 kHz for $H_{dc} = 2000$ Oe and $h_a = 2.2$ Oe. Some fixed temperatures are indicated by symbols. Low T data are close to a Bean critical state, high T data are close to a flux flow regime. Note that in the encircled PE region, no n describes VL dynamics.

critical model. In a typical ac susceptibility experiment as a function of temperature, the $\chi''(\chi')$ curve is not a constant n curve. It will correspond to $n \approx 1$ at high temperatures near the FF regime and to $n \gg 1$ at low temperatures, near the critical state response. However, measurements at fixed T and H and at different frequencies should lie in a constant n curve. We have then performed measurements at several frequencies that are discussed below.

Figure 5 was constructed plotting $\chi''(\chi')$ from experimental non-linear curves $\chi''(T)$ and $\chi'(T)$ for $f = 3$, 10, 30 and 90 kHz. All curves were measured for $H_{dc} = 2000$ Oe and $h_a = 2.6$ Oe (solid lines in the figure). Within these curves, points corresponding to various selected temperatures are plotted with a single symbol for each T. Experimental data are compared with curves predicted by equation (5) for several n (dashed lines in the figure).

It can be seen that at low temperatures, $\chi''(\chi')$ curves approach a Bean model with an effective $J_c(f)$ [7]. It is evident that for the 85 K $\lesssim T \lesssim$ 89 K data (encircled region in the figure) n is not defined; experimental curves are qualitatively different from any theoretical curve calculated using equation (5), indicating an abrupt change in VL dynamics. However, for $T > 89.4$ K (triangles in the figure) a valid n is recovered that decreases rapidly with temperature towards an ohmic regime, with $n = 1$ in the unpinned vortex liquid.

To compare the temperature range between 85 and 89 K, with $T_1(H = 2000$ Oe) and $T_2(H = 2000$ Oe) we go back to figures 3 and 4. Note from figure 3 that $T_2(H_{dc} = 2000$ Oe) $=$ 89.1 K. On the other hand, in figure 4 we have estimated $H_1(86$ K) ~ 1500 Oe, whereas $H_1(84$ K) is not observed for $H < 2000$ Oe, implying that 84 K $< T_1(H = 2000$ Oe) $<$ 86 K. Therefore, the region where there is an abrupt change in the VL dynamics lies between $T_1(H)$ and $T_2(H)$, that is the region of the peak effect.

This result closes the proposed picture. In these YBCO crystals, the PE as a function of H occurs between two

characteristic fields $H_1(T)$ and $H_2(T)$ due to a drastic change in the VL dynamics. This fact coincides with a clear variation in the H dependence of α_L, probably related to a continuos increase in the number of dislocations. In this description, the observed change in the dynamics may be due to a transition from elastic to plastic creep with a larger μ [4], where the relation (5) would no longer be valid.

4. Conclusions

We have explored the static and dynamic behaviour of the vortex lattice in YBCO crystals, in the PE region, at low fields and high temperatures. By performing sensitive linear and non-linear ac susceptibility measurements we have compared the behaviour of the measured critical current and the effective pinning potential wells as a function of temperature, magnetic field and frequency.

For the lower amplitudes, a frequency independent linear Campbell response holds with a very small dissipation. The PE (non-monotonous T dependence) appears only in the non-linear curves with high dissipation, where vortices perform inter-valley motion and an important influence of thermal creep in the response is expected, whereas in the linear Campbell regime no PE in the curvature of the pinning potential wells is observed, in the sense that the measured curves are all monotonous in T.

We conclude that the PE as a function of magnetic field occurs between two characteristic fields $H_1(T)$ and $H_2(T)$. At the first field H_1, the Labusch constant α_L shows an increase with field. This increase may be related to a reduction of the correlation volume due to the increase in the number of VL defects. The sudden change in $\alpha_L(H)$ coincides approximately with the beginning of the anomaly in the slope of the non-linear $\chi'(H)$ curves.

At the second field H_2, the linear real penetration depth grows faster and the linear dissipative component suddenly increases, indicating that dissipative forces prevail over the pinning forces and the Campbell regime is lost. The collapse of the Campbell regime coincides with the minimum observed in the non-linear $\chi'(H)$ curves, indicating the end of the PE region. We interpret this as a signature of the transition to a vortex liquid. The proliferation of defects at H_1 may be related to a continuos transition towards a more disordered phase, previous to the melting transition. Further work is required to dilucidate this matter.

As a function of temperature, at constant magnetic field, we identify two characteristic temperatures $T_1(H_{dc})$ and $T_2(H_{dc})$ as those points where the applied H_{dc} coincides with H_1 and H_2 respectively. Above $T_1(H_{dc})$ there is a continuos reduction of the correlation volume that competes with the intrinsic decrease of α_L with temperature, but is not enough to overcome it. We emphasize that this fact indicates that the PE cannot be ascribed only to an increase in the pining force (i.e. a softening to the VL, allowing a better accommodation to the pinning centres). An additional process must cooperate to enhance the anomaly in the non-linear regime.

We have compared experimental non-linear $\chi''(\chi')$ curves at constant H with theoretical curves predicted for a thin disc in the presence of creep, with a power constitutive relation $E(J)$. The data were extracted from measurements at various frequencies. At low temperatures $\chi''(\chi')$ curves follow a Bean dependence, and above T_2 a transition to an Ohmic regime (characteristic from an unpinned vortex liquid), passing through a highly non-linear dissipative intermediate regime occurs.

However, for $T_1 < T < T_2$ experimental curves are qualitatively different from the predicted theoretical curves indicating that an abrupt change in VL dynamics occurs in the PE region. We find that the dynamics in this region cannot be described within the model, probably due to the relevance of plastic creep.

The smooth behaviour in $\alpha_L(T)$ indicates that there is not a sudden change in the correlation volume at the onset of the PE, as would be expected in a first-order–disorder phase transition at that point. Furthermore, the abrupt increase of dissipative mechanisms at T_2, suggests a transition at the end of the PE. However, we point out that the existence and nature of a phase transition cannot be provided by ac susceptibility measurements, and this issue deserves to be studied further in future.

Summarizing, we propose that the peak effect in YBCO crystals arises from a drastic change in the dynamics between two characteristic H–T lines, $H_1(T)$ and $H_2(T)$. This change is probably due to a continuous increase in the number of dislocations in that region, favoured by a softened VL, before the transition to a vortex liquid occurs.

Acknowledgments

We thank S O Valenzuela and A Moreno for useful discussions and C Chiliotte for technical support. This work was partially supported by UBACyT X200, UBACyT X142, CONICET and Fundación Sauberán.

References

[1] Mikitik G P and Brandt E H 2001 *Phys. Rev.* B **64** 184514
Kierfeld J and Vinokur V 2004 *Phys. Rev.* B **69** 024501
[2] Larkin A I and Ovchinnikov Yu N 1979 *J. Low Temp. Phys.* **34** 409
[3] Higgins M J and Bhattacharya S 1996 *Physica* C **257** 232 and references therein
[4] Kierfeld J, Nordbog H and Vinokur V M 2000 *Phys. Rev. Lett.* **85** 4948
[5] Chandran M, Scalettar R T and Zimányi G T 2003 *Phys. Rev.* B **67** 052507
[6] Chandran M 2004 *Preprint* cond-mat/0407309
[7] Blatter G, Geshkenbein V B and Koopmann J A G 2004 *Phys. Rev. Lett.* **92** 067009
[8] Ravikumar G *et al* 2000 *Phys. Rev.* B **61** 12491
[9] Paltiel Y, Zeldov E, Myasoedov Y N, Shtrikman H, Bhattacharya S, Higgins M J, Xiao Z L, Andrei E Y, Gammel P L and Bishop D J 2000 *Nature* **403** 398
[10] Sobel A, Zeldov E, Rappaport M, Myasoedov Y, Tamegai T, Ool S, Konczykowski M and Geskenbein V B 2000 *Nature* **406** 282
[11] Avraham N *et al* 2002 *Physica* C **369** 36
[12] Gammel P L *et al* 1998 *Phys. Rev. Lett.* **80** 833
Ling X S, Park S R, Mc Clain B A, Choi S M, Dender D C and Lynn J W 2001 *Phys. Rev. Lett.* **86** 712
Park S R, Choi S M, Dender D C, Lynn J W and Ling X S 2003 *Phys. Rev. Lett.* **91** 167003
Gapud A A, Christen D K, Thompson J R and Yethiraj M 2003 *Phys. Rev.* B **67** 104516

[13] Fasano Y, Menghini M, de la Cruz F, Paltiel Y, Myasoedov Y, Zeldov E, Higgins M J and Bhattacharya S 2002 *Phys. Rev.* B **66** 020512(R)
[14] Battacharya S and Higgins M J 1993 *Phys. Rev. Lett.* **70** 2617
Battacharya S and Higgins M J 1995 *Phys. Rev.* B **52** 64
Banerjee S S *et al* 1998 *Physica* C **308** 25
[15] Troyanovski A M, van Hecke M, Saha N, Aarts J and Kes P H 2002 *Phys. Rev. Lett.* **89** 147006
[16] Yeshurum Y, Botemps N, Burlachkov L and Kapitulnik A 1994 *Phys. Rev.* B **49** 1548
Anders S, Parthasarathy R, Jaeger H M, Guptasarma P, Hinks D G and Veen R V 1998 *Phys. Rev.* B **58** 6639
[17] Correa V F, Nieva G and de la Cruz F 2001 *Phys. Rev. Lett.* **87** 57003
[18] Kalisky B, Bruckental Y, Shaulov A and Yeshurun Y 2003 *Phys. Rev.* B **68** 224515
[19] Indenbom M V, Brandt E H, van der Beek C J and Konczykowski M 2004 *Phys. Rev.* B **70** 144525
[20] Divakar U *et al* 2004 *Phys. Rev. Lett.* **92** 237004
[21] D'Anna G, Indenbom M V, Andre M O, Benoit W and Walker E 1994 *Europhys. Lett.* **25** 225
Giapintzakis J, Neiman R L, Ginsberg D M and Kirk M A 1994 *Phys. Rev.* B **50** 16001
Ziese M, Esquinazi P, Gupta A and Braun H F 1994 *Phys. Rev.* B **50** 9491
[22] Pal D, Dasgupta D, Sarma B K, Bhattacharya S, Ramakrishnan S and Grover A K 2000 *Phys. Rev.* B **62** 6699
[23] Stamopoulos D, Pissas M and Bondarenko A 2002 *Phys. Rev.* B **66** 214521
[24] Roy S B, Radzyner Y, Giller D, Wolfus Y, Shaulov A, Chaddah P and Yeshurun Y 2003 *Physica* C **390** 56
[25] Shi J, Ling X S, Lian R, Bonn D A and Hardy W N 1999 *Phys. Rev.* B **60** R12593
[26] Shibata K, Nishizaki T, Sasaki T and Kobayashi N 2002 *Phys. Rev.* B **66** 214518
[27] Safar H, Gammel P L, Huse D A and Bishop D J 1992 *Phys. Rev. Lett.* **69** 824
[28] Worthington T K, Fisher M P A, Huse D A, Toner J, Marwick A D, Zabel T, Feild C A and Holtzberg F 1992 *Phys. Rev.* B **46** 11854
[29] See, for example Henderson W, Andrei E Y and Higgins M J 1998 *Phys. Rev. Lett.* **81** 2352
Xiao Z L, Andrei E Y and Higgins M J 1999 *Phys. Rev. Lett.* **83** 1664
[30] Valenzuela S O and Bekeris V 2000 *Phys. Rev. Lett.* **84** 4200
Valenzuela S O and Bekeris V 2002 *Phys. Rev.* B **65** 060504
[31] Valenzuela S O and Bekeris V 2001 *Phys. Rev. Lett.* **86** 504
[32] Chikumoto N, Konczykowski M, Motohira N and Malozemoff A P 1992 *Phys. Rev. Lett.* **69** 1260
Fuchs D T, Zeldov E, Rappaport M, Tamegai T, Ooi S and Shtrikman H 1998 *Nature* **391** 373
[33] van der Beek C J, Indenbom M V, Ánna G D and Benoit W 1996 *Physica* C **258** 105
[34] Moreno A J, Valenzuela S O, Pasquini G and Bekeris V 2005 *Phys. Rev.* B **71** 132513
[35] Pasquini G, Bekeris V, Moreno A and Valenzuela S O 2004 *Physica* C **408–410** 591
[36] Pasquini G and Bekeris V 2005 *Phys. Rev.* B **71** 014510
[37] Pasquini G and Bekeris V 2004 *Physica* B **354** 257
[38] Aleksandrov I V *et al* 1988 *JETP Lett.* **48** 493
[39] Campbell A M 1971 *J. Phys. C: Solid State Phys.* **4** 3186
Brandt E H 1991 *Phys. Rev. Lett.* **67** 2219
Brandt E H 1992 *Physica* C **195** 1
[40] van der Beek C J, Geshkenbein V B and Vinokur V M 1993 *Phys. Rev.* B **48** 3393
Coffey M W and Clem J R 1992 *Phys. Rev.* B **45** 9872
[41] Brandt E H 1994 *Phys. Rev.* B **50** 13833
[42] Pasquini G, Civale L, Levy P, Lanza H and Nieva G 1997 *Physica* C **274** 165
Pasquini G, Civale L, Lanza H and Nieva G 1999 *Phys. Rev.* B **59** 9627